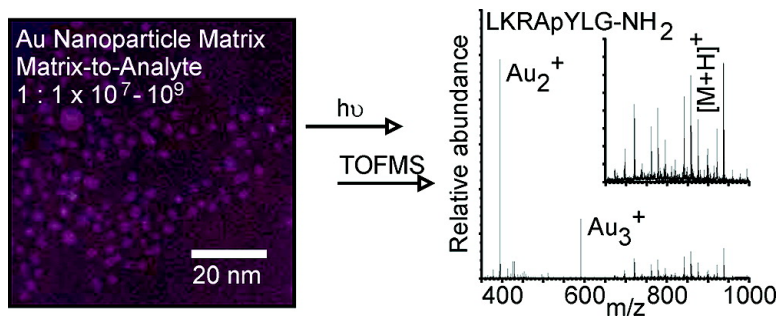


## Size-Selected (2–10 nm) Gold Nanoparticles for Matrix Assisted Laser Desorption Ionization of Peptides

John A. McLean, Katherine A. Stumpo, and David H. Russell

*J. Am. Chem. Soc.*, **2005**, 127 (15), 5304-5305 • DOI: 10.1021/ja043907w • Publication Date (Web): 25 March 2005

Downloaded from <http://pubs.acs.org> on March 25, 2009



### More About This Article

Additional resources and features associated with this article are available within the HTML version:

- Supporting Information
- Links to the 20 articles that cite this article, as of the time of this article download
- Access to high resolution figures
- Links to articles and content related to this article
- Copyright permission to reproduce figures and/or text from this article

[View the Full Text HTML](#)

## Size-Selected (2–10 nm) Gold Nanoparticles for Matrix Assisted Laser Desorption Ionization of Peptides

John A. McLean, Katherine A. Stumpo, and David H. Russell\*

Laboratory for Biological Mass Spectrometry, Department of Chemistry, Texas A&M University, College Station, Texas 77843

Received October 6, 2004; E-mail: russell@mail.chem.tamu.edu

This report describes the first use of size-selected gold nanoparticles (AuNPs) as low concentration ( $1 \text{ AuNP}$  to  $1 \times 10^7$ – $10^9$  analyte molecules) and selective matrixes for the ionization of biomolecules, in contrast with measurements of ions and clusters formed by laser desorption/ionization (LDI) of AuNP.<sup>1</sup> Nanoparticles and, in particular, AuNPs have found wide application in chemical biology (e.g., immunocytochemical probes<sup>2</sup>), and emerging biochemical applications for NP include catalysts for biological reactions,<sup>3</sup> drug encapsulation/targeting,<sup>4</sup> aggregation assays,<sup>5</sup> tunable quantum labels,<sup>6</sup> multiplex encoded quantum taggents,<sup>7</sup> surface enhanced Raman spectroscopy,<sup>8</sup> and analyte concentration prior to mass spectrometry (MS)<sup>9</sup> which are now collectively termed nanobiotechnology.<sup>10</sup> MS applications of metal NPs date back to Tanaka, who demonstrated LDI of intact proteins and protein aggregates by suspending Co particles ( $\sim 30 \text{ nm}$ ), which serve as reservoirs for photon energy deposition, in glycerol.<sup>11</sup> Metal and metalloid (e.g., Ag,<sup>12</sup> C,<sup>13–15</sup> TiN,<sup>15</sup> and Si<sup>16</sup>) substrates offer advantages over organic compounds as matrixes for LDI-MS in terms of sample preparation and flexibility in the sample deposition conditions (e.g., pH, solvents, etc.). Further, the NP size distributions used to date (i.e.  $\sim 10 \text{ nm}$  to  $>2 \mu\text{m}$ ) appear to perform as LDI matrixes independent of irradiation wavelength (near-UV to near-IR), although in all cases, NP sizes are greater than that expected to exhibit quantum effects as described below.

We examined the utility of AuNPs using size distributions of 2, 5, and 10 nm. Transmission electron micrographs (TEM) of 2- and 5-nm AuNPs (Figure 1, data for 10 nm not shown) suggest that the AuNPs are spherical with Sauter mean diameters of 2.65 and 4.46 nm, respectively, which correspond to ca. 250 and 3860 Au atoms/NP.<sup>17</sup> Using AuNPs as LDI matrixes we have successfully ionized a number of peptide systems and small proteins (e.g., bovine insulin,  $M_r = 5733.6 \text{ Da}$ ) including posttranslationally modified peptides (e.g., phosphorylated). Because our proteomics research uses almost exclusively “bottom-up proteomics”, we have not optimized for large proteins. The absorption spectra of the AuNPs contain a broad band from the visible into the ultraviolet, and the characteristic SPR band (owing to coherent oscillation of the AuNP conduction band) appears at ca. 522 nm. For the 2-nm particles, the absence of the SPR band is predicted, owing to the onset of quantum size effects observed for  $\text{NP} < \sim 3 \text{ nm}$ .<sup>18</sup>

When co-deposited with peptides, both positive- and negative-mode MALDI (337 nm) is observed for all three size distributions (Figure 2).<sup>19</sup> In the positive ion spectra  $[\text{M} + \text{H}]^+$ ,  $[\text{M} + \text{Na}]^+$ , and  $[\text{M} + \text{K}]^+$  are observed, as well as peaks corresponding to Au-cluster species (e.g.,  $\text{Au}_3^+$ ,  $\text{Au}_5^+$ ), where the relative abundance of peptide to Au ions ranges from 1.1:1 (2-nm AuNP) to 0.7:1 (10-nm AuNP). The abundance of  $[\text{M} - \text{H}]^-$  ion signals increase as the AuNP size decreases (i.e.,  $2 \text{ nm} > 5 \text{ nm} > 10 \text{ nm}$ ), ranging from a relative abundance of peptide to Au ions of 0.4:1 (2-nm

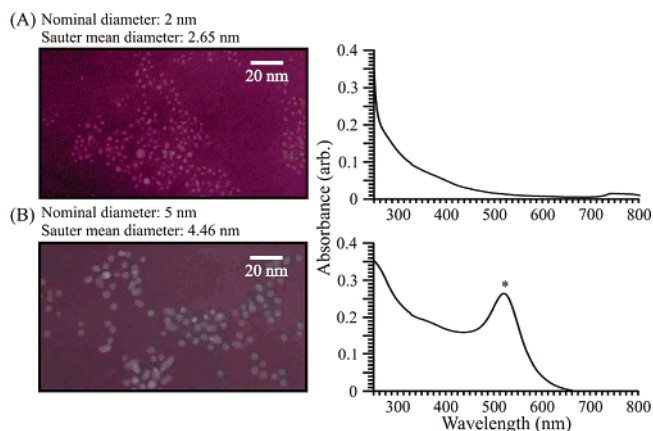


**Figure 1.** TEM images (left) and UV (250–800 nm) solution-phase absorption spectra (right) of (A) 2-nm and (B) 5-nm AuNPs. The surface plasmon resonance band designated by “\*” is observed in spectra of all particles  $>3 \text{ nm}$ .

AuNP) to no peptide ions observed using 10-nm AuNP. The abundances of higher-order Au-clusters increase as AuNP size increases (i.e.,  $10 > 5 > 2 \text{ nm}$ ). In general, spot-to-spot precision of  $<10\%$  RSD in signal intensity across the deposited material is observed with limits of detection ca. 100 fmol of peptide deposited.

Prior studies using metal and metalloid substrates have utilized materials exhibiting macroscopic properties of the bulk material.<sup>11–16</sup> Energy transfer from the substrate to the analyte likely occurs via a thermally driven process, similar to the mechanism proposed by Tanaka,<sup>11</sup> and abundant Au-cluster ions in the spectra of 5- and 10-nm AuNPs are consistent with this idea. For all size distributions utilized here, the calculated heat diffusion length ( $d_{\text{diff}}$ ) is  $\sim 3$  orders of magnitude (ca.  $1.43 \mu\text{m}$ ) longer than the NP diameter, thus the entire NP volume effectively achieves the same temperature and the corresponding change in surface temperature  $\Delta T$  is  $\gg 1 \times 10^4 \text{ K}$ .<sup>20</sup> However, this explanation does not account for the different ion yields from 2-nm AuNPs. With decreasing size, the AuNPs begin to exhibit meso- and microscopic properties, which exhibit quantum confinement effects and are thus termed quantum dots (QDs).<sup>21</sup> For 2-nm AuNPs it appears that energy transfer involves electronic excitation,<sup>22</sup> and analyte ionization is a result of such processes.

AuNP matrixes also afford selectivity which is not observed using organic matrixes. For example, the preferential ionization of phosphotyrosine (pTyr)- over phosphoserine (pSer)- or phosphothreonine (pThr)-containing peptides. Phosphotyrosine is important for many cell regulatory functions, but pTyr analysis is challenging owing to the low abundance of phosphorylation at Tyr ( $<0.5\%$ ) relative to that at Ser and Thr. Thus, the development of selective method-

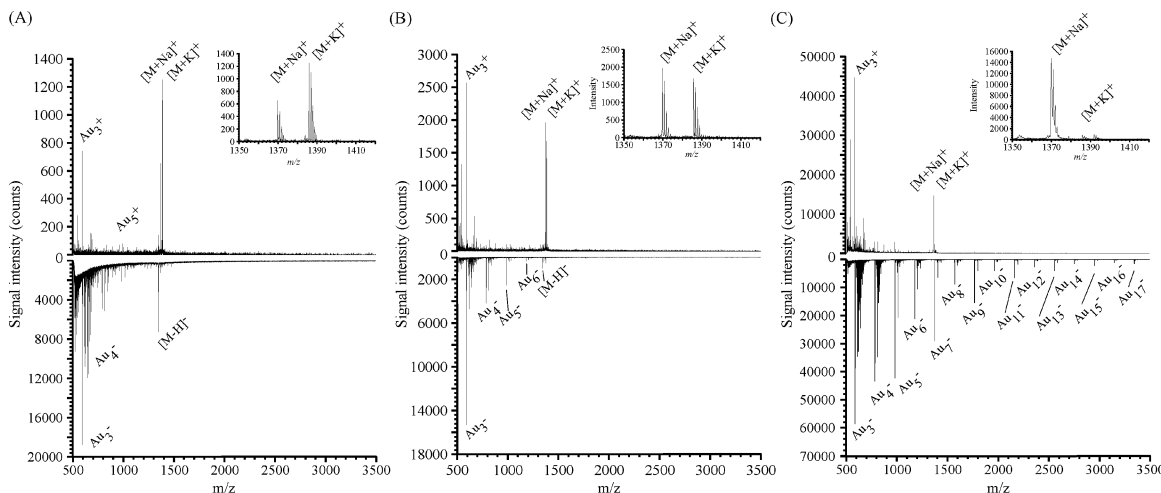


**Figure 2.** MALDI-TOFMS mass spectra of substance P (RKPQFFGLM-NH<sub>2</sub>,  $M_r = 1347.64$  Da) obtained by using AuNPs: (A) 2 nm, (B) 5 nm, and (C) 10 nm (337 nm, energies of ca. 120 and 180  $\mu\text{J pulse}^{-1}$  for positive and negative mode MALDI, respectively). AuNP/peptide molar ratio ranged from  $1:1 \times 10^7$ – $10^9$ .

ologies for determining pTyr in a background of pSer and pThr is the subject of much recent work.<sup>23</sup> By using AuNPs as matrixes for an equimolar ratio of phosphopeptides (i.e., LKRApYLG-NH<sub>2</sub>, LRRApSLG, and LKRApTLG-NH<sub>2</sub>), only ions corresponding to LKRApYLG-NH<sub>2</sub>, viz.  $[\text{M} + \text{H} - \text{PO}_3]^+$ ,  $[\text{M} + \text{H}]^+$ , and cationized species are observed, whereas high-abundance ions for pSer and pThr species only result when they are analyzed separately. We are performing additional studies to understand the molecular interaction responsible pTyr selectivity but presently rationalize this as cation- $\pi$  interactions akin to those observed between AuNPs and aromatic molecules.<sup>24</sup>

In comparison with conventional UV MALDI using organic matrixes,<sup>25</sup> the molar matrix-to-analyte (M/A) ratio for AuNP MALDI is ca.  $1 \text{ NP}/1 \times 10^7$ – $10^9$  analyte molecules vs  $1 \times 10^3$ – $10^5$ /analyte molecule. The observed M/A suggest a highly efficient ionization process for AuNPs whereby AuNPs may possess the capacity for ionization of more than one analyte per laser pulse, or the potential for regeneration to a matrix-“active” state between laser pulses. This apparent inversion in the optimum M/A ratio also corroborates results recently obtained from samples (peptide film and tissue) implanted with massive gold clusters (i.e., Au<sub>400</sub><sup>+</sup>).<sup>26</sup>

The use of QDs as matrixes for biological MS opens several exciting avenues for defining new experimental constructs in life sciences research: (i) conjugated QDs to elicit analyte selectivity prior to MS analysis<sup>9</sup> with inherent matrix capabilities, (ii) in vivo introduction of QDs via receptor-mediated endocytosis<sup>27</sup> or phospholipid micelles<sup>28</sup> followed by “tagless” imaging-mode MS, (iii) immobilized QDs as biomolecular arrays followed by SPR and MS readout, and (iv) tailoring the optoelectronic properties of NPs or QDs for specific MS applications by changing size, shape, composition, or derivatization.<sup>6,29</sup> Importantly, the enhanced matrix ionization efficiency of AuNP over organic matrixes (indicated by a reduction in M/A ratios of 10–14 decades) provides a means for matrix incorporation (with potential selectivity) without adulteration of the sample or toxicity for in vivo experiments.

**Acknowledgment.** This work was supported by the Department of Energy, Division of Chemical Sciences, BES (DE-FG03-95ER14505) and the National Institutes of Health (1R01 RR01958701).

## References

- (1) Schaaff, T. G. *Anal. Chem.* **2004**, *76*, 6187.
- (2) Faulk, W. P.; Taylor, G. M. *Immunochemistry* **1971**, *8*, 1081.
- (3) Xiao, Y.; Patolsky, F.; Katz, E.; Hainfeld, J. F.; Willner, I. *Science* **2003**, *299*, 1877.
- (4) Akerman, M. E.; Chan, W. C. W.; Laakkonen, P.; Bhatia, S. N.; Ruoslahti, E. *Proc. Natl. Acad. Sci. U.S.A.* **2002**, *99*, 12617.
- (5) Nam, J.-M.; Thaxton, C. S.; Mirkin, C. A. *Science* **2003**, *301*, 1884.
- (6) Han, M.; Gao, X.; Su, J. Z.; Nie, S. *Nat. Biotechnol.* **2001**, *19*, 631.
- (7) Bruchez, M.; Moronne, M.; Gin, P.; Weiss, S.; Alivisatos, A. P. *Science* **1998**, *281*, 2013.
- (8) Mulvaney S. P.; Musick, M. D.; Keating, C. D.; Natan, M. J. *Langmuir* **2003**, *19*, 4784.
- (9) Teng, C.-H.; Ho, K.-C.; Lin, Y.-S.; Chen, Y.-C. *Anal. Chem.* **2004**, *76*, 4337.
- (10) Penn, S. G.; He, L.; Natan, M. J. *Curr. Opin. Chem. Biol.* **2003**, *7*, 609.
- (11) Tanaka, K.; Waki, H.; Ido, Y.; Akita, S.; Yoshida, Y.; Yoshida, T. *Rapid Commun. Mass Spectrom.* **1988**, *2*, 151.
- (12) Owega, S.; Lai, E. P. C.; Bawagan, A. D. O. *Anal. Chem.* **1998**, *70*, 2360.
- (13) Sunner, J.; Dratz, E.; Chen, Y.-C. *Anal. Chem.* **1995**, *67*, 4335.
- (14) Dale, M. J.; Knochenmuss, R.; Zenobi, R. *Anal. Chem.* **1996**, *68*, 3321.
- (15) Schürenberg, M.; Dreisewerd, K.; Hillenkamp, F. *Anal. Chem.* **1999**, *71*, 221.
- (16) Wei, J.; Buriak, J. M.; Siuzdak, G. *Nature (London)* **1999**, *399*, 243.
- (17) TEM images were obtained using a JEOL JEM-2010 instrument with 200 kV electrons at  $4 \times 10^5$  magnification. Sauter mean diameter ( $D_{3,2}$ ) is defined as  $D_{3,2} = (\sum n_i d_i^3) / (\sum n_i d_i^2)$ .
- (18) Daniel, M.-C.; Astruc, D. *Chem. Rev.* **2004**, *104*, 293.
- (19) MALDI-TOFMS was performed on an Applied Biosystems Voyager DE STR equipped with a Spectra-Physics N<sub>2</sub> laser for MALDI at 337 nm.
- (20) Calculations for AuNP were performed analogous to that described in ref 15, namely:  $d_{\text{diff}} \approx 2(\tau_L \lambda_w / \rho c)^{1/2}$  and  $\Delta T = H / \rho c d$ . Where  $\tau_L$  is laser pulse duration,  $H$  is laser fluence,  $\lambda_w$  is heat conductivity,  $\rho$  is density, and  $c$  is specific heat. Values for Au were obtained from *CRC Handbook of Chemistry and Physics*, 76th ed.; Lide, D. R., Ed.; CRC Press: FL, 1996.
- (21) Schmid, G. In *Encyclopedia of Nanoscience and Nanotechnology*; Nalwa, H. S., Ed.; American Scientific Publishers: CA, 2004; Vol. 5, p 387.
- (22) Robinson, G. W.; Frosch, R. P. *J. Chem. Phys.* **1963**, *38*, 1187.
- (23) Salomon, A. R.; Ficarro, S. B.; Brill, L. M.; Brinker, A.; Phung, Q. T.; Ericson, C.; Sauer, K.; Brock, A.; Horn, D. M.; Schultz, P. G.; Peters, E. C. *Proc. Natl. Acad. Sci. U.S.A.* **2003**, *100*, 443.
- (24) Kumar, A.; Mandal, S.; Mathew, S. P.; Selvakannan, P. R.; Mandale, A. B.; Chaudhari, R. V.; Sastry, M. *Langmuir* **2002**, *18*, 6478.
- (25) Karas, M.; Hillenkamp, F. *Anal. Chem.* **1988**, *60*, 2299.
- (26) (i) Novikov, A.; Caroff, M.; Della-Negra S.; Lebeyec, Y.; Pautrat, M.; Schultz, J. A.; Tempez, A.; Wang, H.-Y. J.; Jackson, S. N.; Woods, A. S. *Anal. Chem.* **2004**, *76*, 7288. (ii) Tempez, A.; Ugarov, M.; Egan, T.; Schultz, J. A.; Novikov, A.; Della-Negra, S.; Lebeyec, Y.; Pautrat, M.; Caroff, M.; Smentkowski, V. S.; Wang, H.-Y. J.; Jackson, S. N.; Woods A. S. *J. Proteome Res.* **2005**. In press.
- (27) Chan, W. C. W.; Nie, S. *Science* **1998**, *281*, 2016.
- (28) Dubertret, B.; Skourides, P.; Norris, D. J.; Noireaux, V.; Brivanlou, A. H.; Libchaber, A. *Science* **2002**, *298*, 1759.
- (29) Prodan, E.; Radloff, C.; Halas, N. J.; Nordlander, P. *Science* **2003**, *302*, 419.

JA043907W